Quiescence induced by iron challenge protects neuroblastoma cells from oxidative stress

Casilda V. Mura,*,[1] Ricardo Delgado,*,† Pabla Aguirre,* Juan Bacigalupo*,† and Marco T. Núñez*,†

*Department of Biology, Faculty of Sciences and †Cell Dynamics and Biotechnology Research Center, University of Chile, Santiago, Chile

Abstract

The brain uses massive amounts of oxygen, generating large quantities of reactive oxygen species (ROS). Because of its lipid composition, rich in unsaturated fatty acids, the brain is especially vulnerable to ROS. Furthermore, oxidative damage in the brain is often associated with iron, which has pro-oxidative properties. Iron-mediated oxidative damage in the brain is compounded by the fact that brain iron distribution is non-uniform, being particularly high in areas sensitive to neurodegeneration. This work was aimed to further our understanding of the cellular mechanisms by which SHSY5Y neuroblastoma cells adapt to, and survive increasing iron loads. Using an iron accumulation protocol that kills about 50% of the cell population, we found by cell sorting analysis that the SHSY5Y subpopulation that survived the iron loading arrested in the G_0 phase of the cell cycle. These cells expressed neuronal markers, while their electrical properties remained largely unaltered. These results suggest that upon iron challenge, neuroblastoma cells respond by entering the G_0 phase, somehow rendering them resistant to oxidative stress. A similar physiological condition might be involved in neuronal survival in tissues known to accumulate iron with age, such as the hippocampus and the *substantia nigra pars compacta*.

Keywords: cell cycle, iron, neuroblastoma cells, oxidative stress, quiescence

The brain accounts for 20% of the oxygen consumed by the human body, even though it comprises only 2% of the body weight (Sokoloff 2000). Oxygen consumption is accompanied by the generation of large quantities of reactive oxygen species (ROS) during oxidative phosphorylation in the brain. This organ is thought to be especially vulnerable to ROS, since it is rich in lipids with unsaturated fatty acids, the targets of lipid peroxidation (Bazan 2003). In fact, studies of human post-mortem brain tissue have implicated oxidative stress in neuronal death, particularly in neurodegenerative disorders. Increases of various biomarkers of oxidative stress have been observed in diseased regions of post-mortem brain tissues from patients with Alzheimer, Parkinson's and Huntington's diseases, as well as prion disorders and progressive supranuclear palsy (Jenner and Olanow 1996; Andersen 2004; Barnham 2004; Hald and Lotharius 2005). In contrast to other tissues where damaged cells are replaced, a loss of neurons in the adult brain is largely irreversible. Yet, the brain is able to adapt to oxidative stress and function during the lifespan of humans.

Iron is a pro-oxidant involved in the generation of oxidative damage (Sayre *et al*. 2000). Brain iron homeostasis is unique among organs because of the non-uniform distribution of iron in its different regions and cell types (Zecca *et al*. 2004). In particular, high iron content has been reported in some brain areas sensitive to neurodegeneration (Youdim and Riederer 1993; Griffiths *et al*. 1999). Because of their post-mitotic condition, neurons cannot reduce intracellular iron by cell division and depend entirely on the mechanism of cellular iron homeostasis to control iron levels. Despite increased iron content with age (Zecca *et al*. 2001; Gotz *et al.* 2004), a large proportion of neuronal cells manage to stay viable and to control the degree of oxidative

Address correspondence and reprint requests to Dr C.V. Mura, Ophthalmology Department, Tufts New England Medical Center, 750 Washington St., Boston MA 02111, USA. Email: cmura@tufts-nemc.org

[1]Current address: Ophthalmology Department, Tufts New England Medical Center, 750 Washington St., Boston MA 02111, USA

Abbreviations used: DMEM, Dulbecco's modified Eagle medium; LC, *locus coeruleus*; NM, neuromelanine; PBS, phosphate- buffered saline; PI, propidium iodine; ROS, reactive oxygen species; SN, *substantia nigra*.

damage, presumably through the activation of adaptive mechanisms. Increased iron levels are accompanied by increases in ROS and lipid peroxidation, whereas treatment with the Fe chelator desferrioxamine results in reduction of the neurological symptoms induced by iron (Doraiswamy and Finefrock 2004).

The various neuronal cell types seem to respond differentially to iron accumulation. Recent studies of metal-related neuronal vulnerability conducted on two human brainstem nuclei, the *locus coeruleus* (LC) and *substantia nigra* (SN), illustrate this point. While LC and SN share anatomical and biochemical similarities, being both pigmented due to the presence of neuromelanine (NM), and better undergoing degeneration in Parkinson's disease, the SN neurons are more vulnerable than those from the LC in pathological conditions where iron-mediated oxidative stress plays an important role (Zecca *et al*. 2004). Relevant information is provided by the characterization of a newly established neuronal ρ-0 cell line, which accumulates iron and other metals and is highly susceptible to oxidative stress (Fukuyama *et al*. 2002). Recently, it was reported that iron accumulation produces oxidative stress and oxidative damage in neuroblastoma cells (Núñez-Millacura *et al*. 2002; Aguirre *et al*. 2005). Neuroblastoma cells that adapt to a high iron load down-regulate the expression of the iron importer Divalent Metal transporter (DMT1), and at the same time up-regulate the expression of the iron exporter Iron regulated gene 1 (Ireg1) and of the iron-storage protein ferritin (Aguirre *et al*. 2005). Thus, the differential capacity of neuronal subtypes to co-ordinately regulate the expression of iron transporters may be one of the clues to successful adaptation. Similarly, part of the adaptation process includes increased glutathione synthesis and increased activity of glutathione peroxidase and glutathione transferase (Núñez *et al*. 2004).

This work was aimed to further understanding of the cellular mechanisms by which SHSY5Y neuroblastoma cells adapt and survive to increasing iron loads. Using an iron accumulation protocol that kills about 50% of the cell population, we found that surviving SHSY5Y cells accumulated in the G_0 phase of cell cycle, and expressed markers of neuronal differentiation, while their electrical properties remained largely unaltered. These results provide insights into the processes of neuronal degeneration and survival in tissues known to accumulate iron with age, such as the hippocampus and the *susbtantia nigra pars compacta*.

Materials and methods

Cell culture and iron treatment

Human neuroblastoma SHSY5Y cells (CRL-2266, American Type Culture Collection Rockville, MD, USA) is a well established cell line, corresponding to a third successive subclone of the SK-N-SH line originally established from a bone marrow biopsy of a neuroblastoma patient. The parental cell line comprises at least two morphologically different phenotypes, neuroblastic (N-type) and substrate adherent (S-type), which can undergo trans-differentiation (Ross *et al*. 1983). SHSY5Y cells can differentiate into cells with neuronal morphology, the phenotype of which varies depending on the inducing agent (Pahlman *et al*. 1995; Encinas *et al*. 2000). SHSY5Y cells were seeded at 1×10^4 cells per 1 cm^2 plastic wells, cultured in MEM/F12 medium supplemented with 10% fetal bovine serum and 5 mM glutamine, and incubated in a 5% CO_2 atmosphere. The medium was replaced every three days. Under these conditions, doubling time was 48 h. The total iron concentration of this medium was 7.03 μM as determined by atomic absorption spectrometry. The culture reached a steady-state number of cells after 8 days. At this time, cells were cultured for 2 days in DMEM/F12 supplemented with iron, offered as a $FeCl_3$-Na nitrilotriacetate complex (NTA 1 : 2.2 mol:mol) in the amount needed to reach the desired iron concentration. Low (2 μM) iron medium was obtained by adding 5 μM of the strong iron chelator desferrioxamine to the standard 7 μM Fe medium. The iron concentrations mentioned in the text correspond to total iron. The high affinity constant of the Fe-NTA complex 9log K: 30.4; Martell and Smith 2004) indicates that the free Fe^{3+} concentration should be considerably lower.

Cell viability

Cell respiration, an indicator of cell viability, was assessed by the mitochondrial-dependent reduction of 3-(4,5-dimethylthiazol-2-yl)-2.5-diphenyltetrazolium bromide (MTT) to formazan (Gross and Levi 1992). Cells were cultured in 96-well dishes and subjected to the progressive iron accumulation protocol as above. At the end of each experiment, cell viability was measured using the MTT proliferation Assay Kit (Molecular Probes, Eugene, OR, USA), following the instructions of the manufacturer. The extent of the formazan production was determined by measuring optical density at 650 nm in a Tecan Sunrise microplate reader (Tecan, Grödig/Salzburg, Austria). Experimental points were tested in triplicates.

Total cell iron content

SHSY5Y cells were cultured at a density at 1×10^4 cells per 1 cm^2 plastic well for 8 days, followed by incubation for 2 days in DMEM/F12 supplemented with varied amounts of iron. Total iron content was determined by atomic absorption spectrometry (Perkin Elmer Model 2280, Norwalk, CT).

Cell cycle analysis and determination of quiescent G_0 cells

SHSY5Y cells were cultured at 1×10^4 cells per 1 cm^2 plastic well for 8 days, followed by incubation for 2 days in Dulbecco's modified Eagle medium (DMEM)/F12 supplemented with varied amounts of iron. For cell cycle analysis, cell aliquots were labeled with propidium iodine (PI, 10 mg/mL, Sigma, St. Louis, MO, USA), treated with RNAse A (100 μg/mL, Sigma) and their DNA content analyzed on a Fluorescence Activated Cell Sorter flow cytometer (Becton Dickinson, San Jose, CA, USA) equipped with MODFIT software. Content of quiescent (G_0) cells was assessed in cell aliquots after staining with Rhodamine 123 (Rho, 5 μM, Sigma) plus PI, followed by flow cytometric analysis by using the CELLQUEST software. Quiescent G_0 status refers to alive cells exhibiting a low

Rho (PI-/Rho low) fluorescence signal (Wolf *et al*. 1993), due to scarce mitochondrial oxidative metabolism (Kim *et al*. 1998).

Immunofluorescence of SHSY5Y cells

SHSY5Y cells were cultured at 1×10^4 cells per 1 cm^2 plastic well for 8 days, followed by incubation for 10 days in DMEM/F12 supplemented with varied amounts of iron. The immunofluorescence was done according to a procedure previously described (Mura *et al*. 2004). Briefly, cells were attached to glass cover slips coated with 10 μg/mL poly-L-lysine. For staining, they were washed three times in phosphate-buffered saline (PBS) and then fixed with a freshly prepared 4% paraformaldehyde in PBS. Fixed cells were washed five times in PBS and permeabilized with 0.2% Triton in PBS. The non-specific protein binding sites were blocked by incubation in PBS containing 0.2% gelatin (gelatin-PBS). Cells were then incubated with the primary antibody diluted in gelatin-PBS at room temperature (23–25°C) for 1 h, washed with gelatin-PBS six times for 30 min and incubated with the appropriate secondary antibody for 1 h. After washing as described, cells were mounted in Gelvatol (10% glycerol, Dabco, azide 0,1%). Immunofluorescence of SHSY5Y cells was viewed in a Zeiss Axiovert 200 M epifluorescence microscope (Carl Zeiss AG, Oberkochen, Germany) equipped with temperature and CO_2 controllers. Images of low magnification fields from each culture were acquired with an Axiocam HR camera (Carl Zeiss) attached to a PC equipped with Axiovision software (Carl Zeiss). A shutter and a neutral density filter were used to minimize photo bleaching. Fluorescence intensity from at least 100 cells from the captured images was determined using the QUANTITY ONE (Bio-Rad, Hercules, CA, USA) software. Fluorescence values were expressed as arbitrary fluorescence intensity units.

Electrophysiology

Whole cell currents from control SHSY5Y cells (7 μM Fe) and cells subjected to different iron treatments were recorded with the patch-clamp technique under voltage-clamp mode, using an Axopatch 1D amplifier (Axon Instruments, Inc., Union City, CA). The currents were evoked by depolarizing pulses from a holding potential of −80 mV. The cells were bathed with a solution containing (in mM) 150 NaCl, 2.5 KCl, 1 $CaCl_2$, 1.5 $MgCl_2$, 10 Hepes, pH 7.6. The pipette solution contained (in mM): 120 KCl, 2 $MgCl_2$, 1 $CaCl_2$ 10 EGTA, 4 ATP and 10 HEPES, pH 7.6. The recorded currents were acquired in a PC using a LabMaster interface (Scientific Solutions, Solon, Ohio 44139) and analyzed using pCLAMP 6.0 Software (Axon Instruments).

Data analysis

Variability across experiments was < 20%. One-way ANOVA was used to test statistical differences in mean values and Student-Newman-Keuls post-hoc test was used for comparisons (IN STAT program from GraphPad Prism, San Diego, CA 92130 USA). Differences were considered significant if $p < 0.05$.

Results

SHSY5Y cells accumulate iron when exposed to high iron concentrations

Fe accumulation was determined in cells previously grown to confluence for eight days and challenged for an extra two days in medium containing 2–300 μM Fe (Fig. 1). Total cell iron content after the initial eight days of culture was 4.27 ± 1.35 pmol/mg of protein. After two extra days, the cells cultured in media containing 2–80 μM Fe exhibited a slight iron accumulation, although there were no significant statistical differences among them. Significant differences in iron content were observed between 2 and 125 μM Fe ($p < 0.05$), 2 and 300 μM Fe ($p < 0.01$), and 7 and 300 μM Fe ($p < 0.05$).

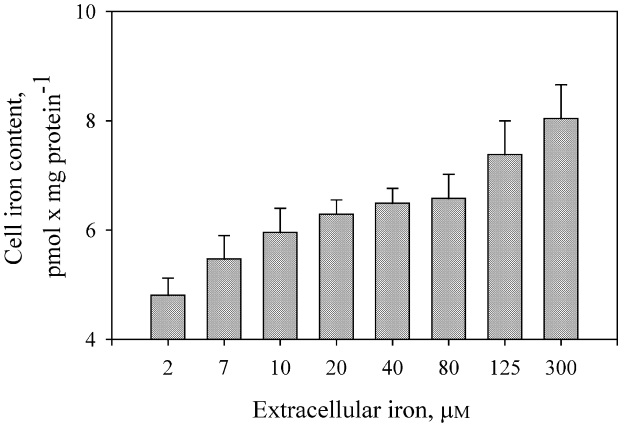

Fig. 1 Fe content of SHSY5Y cells subjected to different iron treatment. SHSY5Y cells were grown for 8 days and then challenged for 2 days with different Fe concentrations, from 2 to 300 μM. Total Fe content was determined by mass spectrometry. Data are mean ± SEM values of 4 independent determinations. Significant differences in iron content were observed between 2 and 125 μM ($p < 0.05$), 2 and 300 μM ($p < 0.01$), and 7 and 300 μM groups ($p < 0.05$).

Iron treatment leads to neuronal cell death, although a sub-population of cells survives

To determine whether iron retention was linked to loss in cell viability, we evaluated the viability of cells subjected to different amounts of iron in the culture medium for various time points. The viability of SHSY5Y cells treated with iron decreased both as a function of iron concentration and time in culture (Fig. 2). Viability decreased by more than 50% when cells were challenged for 2 days with iron concentrations of 80 μM or higher. After two days of treatment, the difference in viability between cells challenged with 7 or 20 μM Fe compared to those treated with 80, 125 and 300 μM Fe was significant ($p < 0.005$). Cell viability tended to stabilize with time, between 2 and 8 days in culture. Nevertheless, a slight decrease in viability was found for the higher iron conditions between day 8 and day 10 of culture. However, even under the most extreme iron loading conditions (300 μM Fe for 10 days), a sub-population of cells managed to remain viable. Cell viability assayed by MTT reduction was confirmed by flow cytometry (not shown). Both methods confirmed the loss of viability at 125 and 250 μM Fe after two days of iron treatment.

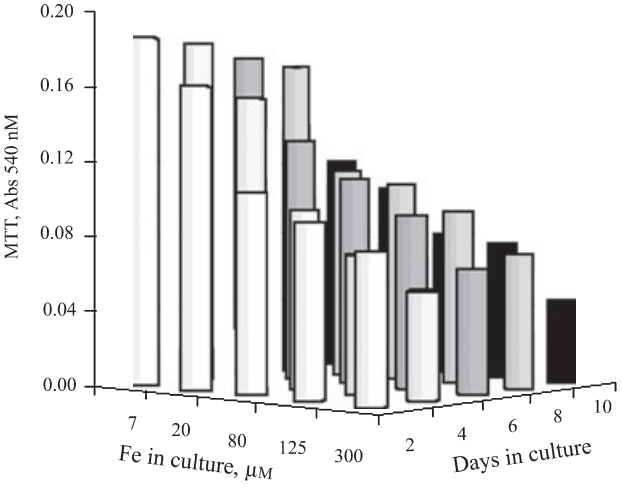

Fig. 2 Viability of SHSY5Y cells subjected to different iron treatment. MTT reduction by SHSY5Y cells in the presence of increasing iron concentrations at different times. Exponentially growing cells were treated with the indicated Fe concentration for 2, 4, 6, 8 and 10 days. Cell growth inhibition was assessed as described in Material and methods. Data corresponds to mean ± SEM (bars) values of 3 observations from independent assays in triplicates. At 2, 4, and 8 days of iron treatment, cells cultured with 80, 125 and 300 μM iron concentrations showed a significant difference with the control group, at 7 μM iron: $p < 0.005$, at 10 days these differences were also significant with the control group with a $p < 0.01$. At two days of treatment, differences between 7, 20 and 80 μM with the 125 and 300 μM were also significant: $p < 0.005$.

High iron induced entrance into G_0

To advance our understanding of the processes by which SHSY5Y cells adapt to a high iron load, the cellular proliferative status was analyzed by cell sorting after treatment with different Fe concentrations in the culture medium (Fig. 3). SHSY5Y cell populations selected as Rho-123^{low} were comprised predominantly of quiescent cells, while Rho-123^{high} cells contained high numbers of cycling cells. When SHSY5Y cells were treated for 2 days with 7 μM Fe, about 30% of the population was Rho-123^{low} and 70% was Rho-123^{high}. When exposed to 80 μM Fe, the distribution between Rho-123^{low} and Rho-123^{high} was 41% and 59%, while at 250 μM Fe, it was 52% and 48%, respectively (Fig. 3a). The SHSY5Y cell population in G_0 increased after 2 days of 250 μM Fe treatment (Fig. 3b). The difference between 5 and 250 μM Fe samples was statistically significant ($p < 0.01$). Thus, iron accumulation induced the cells to enter into a quiescent state.

SHY5Y cells subjected to different Fe concentrations express markers of neuronal differentiation

The morphology of SHSY5Y cells treated for 10 days with high Fe concentrations resembled primary neurons under phase contrast microscopy, an indication that high iron may be triggering a differentiation program. To determine whether

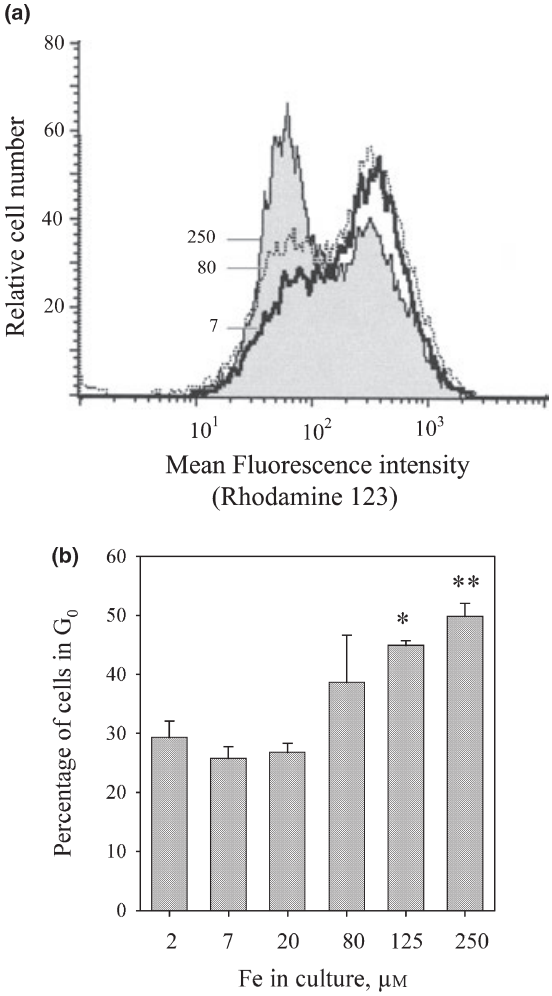

Fig. 3 Cell Cycle analysis of SHSY5Y cells subjected to different iron treatment. (a) SHSY5Y cells were grown for 8 days and then challenged for 2 days with 2, 7, 20, 80, 125 or 250 μM Fe. The proportion of cells in G_0, defined as those exhibiting minimal RNA content and uniform DNA content, giving a low Rho (PI-/Rho^{low}) fluorescence signal, was assessed as described in Material and methods. (b) The relative percentage of cells in G_0 was calculated from four independent experiments. A statistically significant difference was found between the 7 μM and the 125 μM (*$p < 0.05$) and 250 μM (**$p < 0.01$) samples.

SHSY5Y cells were shifting to a neuronal phenotype, the expression of the neuron-specific markers MAP2 and tau were evaluated by immunofluorescence. MAP2 reactivity was localized both to the cell body and to short processes. Fluorescence intensity paralleled the Fe concentration in the medium, whereas cells subjected to 2 μM Fe showed no MAP2-associated fluorescence (Fig. 4a). A clear change in the phenotype was apparent between 2 μM to 7 μM or higher iron concentrations. The cells grown in 2 μM Fe presented a rounded, undifferentiated phenotype, while cells cultured in 7–250 μM Fe adopted a more neuron-like phenotype (Fig. 4a). Quantification of MAP-2 associated fluorescence

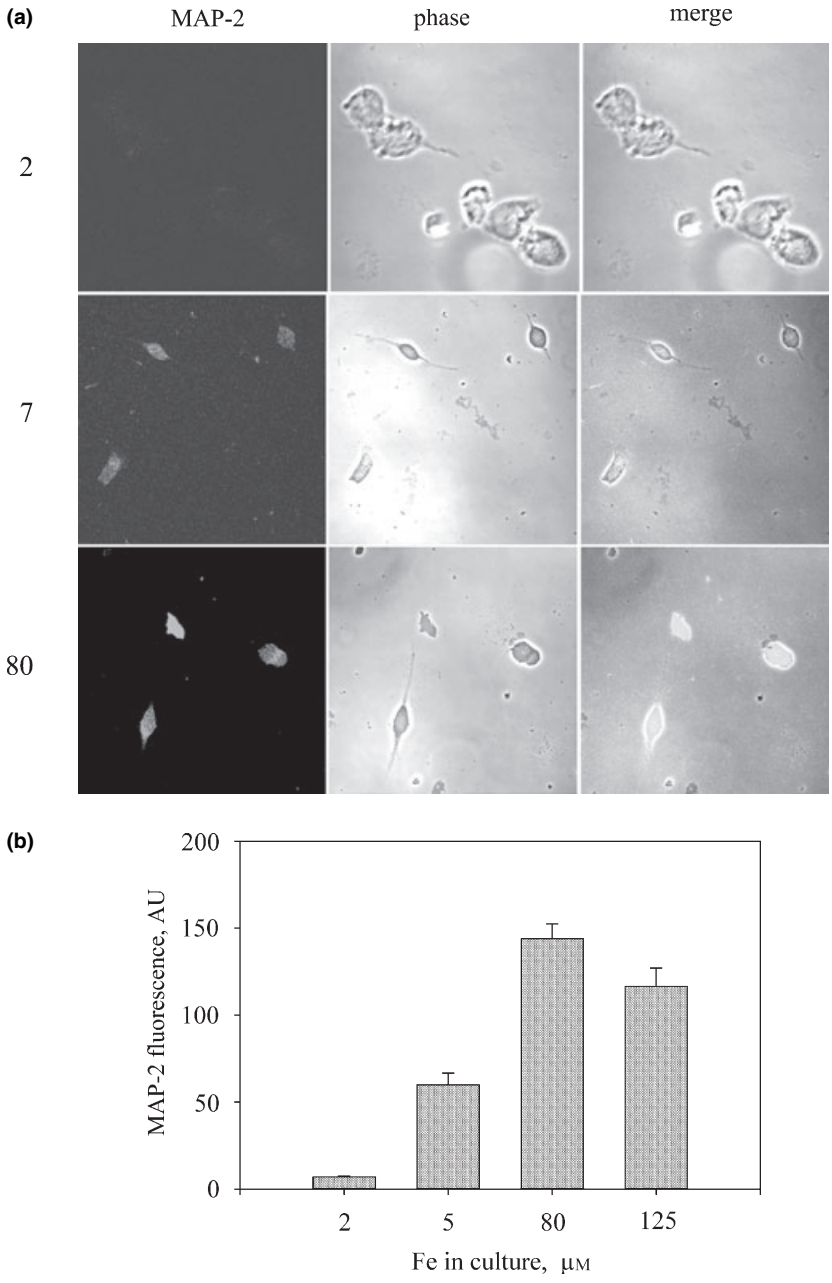

Fig. 4 MAP2 immunofluorescence in SHSY5Y cells. (a) Cells grown for 8 days and then challenged for 10 days with different iron concentrations. Cells were fixed, permeabilized, and incubated with a rabbit polyclonal anti-MAP2 antibody followed by Alexa Fluor 488 goat antirabbit IgG. Fluorescence values were expressed as arbitrary fluorescence intensity units. Bar −25 μm. (b) Quantitative analysis of MAP-2 fluorescence. Cell fluorescence intensity was determined using Quantity One software in at least 100 cells for each iron concentration. Abscise values represent mean fluorescence ± SD, in arbitrary units.

indicated that iron in the 80–125 μM range induced a 15–20 fold increase in MAP-2 expression compared to 2 μM (Fig. 4b). Tau immunoreactivity presented a distribution similar to MAP-2, although it was evident even at lower Fe (2 μM, data not shown). Thus, in parallel with proliferative quiescence, iron induced a differentiated neuronal phenotype.

Electrical properties are not altered in SHSY5Y cells adapted to high Fe exposure

To investigate the effects of iron exposure on the functionality of SHSY5Y cells treated for 10 days with different Fe concentrations, the electrophysiological properties of iron-treated cells were examined. We compared the amplitude of the whole cell currents evoked by depolarizing voltage pulses in cells subjected to different iron treatments (Fig. 5a). We also determined, under current-clamp conditions, whether Fe treatment altered their resting potentials. The voltage-dependent inward currents were virtually identical in cells treated with iron concentrations above 7 μM. The average inward current amplitude evoked by a 60 mV depolarizing step from −80 mV (holding potential) were −200 ± 47 pA ($n = 14$) at 2 μM Fe and −189 ± 63 pA ($n = 9$) at 7 μM Fe. At higher iron concentrations, 80, 125, and 250 μM, the current amplitudes were −114 ± 55 pA ($n = 6$); −187 ± 88

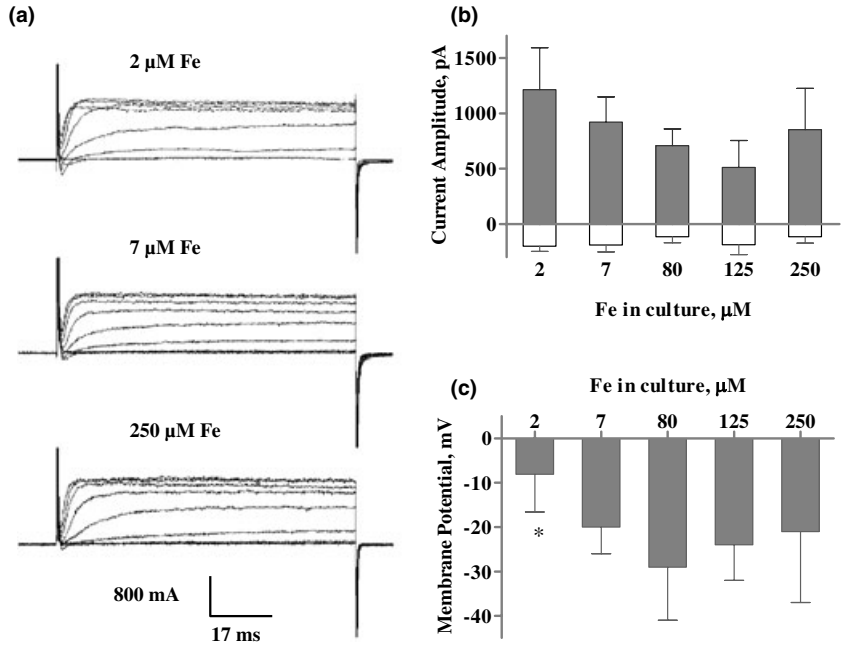

Fig. 5. Electrophysiology of SHSY5Y cells subjected to different iron concentrations. SHSY5Y cells were grown for 8 days and then challenged for 10 days with culture media containing iron concentrations between 2 and 250 μM, after which they were characterized in their basic electrical properties: whole-cell currents and membrane potential. (a) Shows representative whole cell current families obtained at three different iron concentrations, evoked by a 10 mV depolarizing voltage steps protocol from −80 mV holding potential up to 20 mV. (b) Shows a histogram comparing the inward (white bars) and outward (grey bars) amplitudes. (c) Shows the values of membrane potential measured in current clamp conditions of cells subjected to different Fe concentrations. Values are mean ± SD of 6–12 determinations for each value. *, significantly different ($p < 0.05$) than control (7 μM Fe) condition.

pA ($n = 4$) and -115 ± 57 pA ($n = 8$), respectively (Fig. 5b, white bars). These values are not significantly different ($p < 0.05$) than at 7 μM Fe. Values for the outward current amplitudes were 1213 ± 380 pA ($n = 12$), 922 ± 225 pA ($n = 10$), 708 ± 151 pA ($n = 6$), 512 ± 243 pA ($n = 5$) and 853 ± 373 pA ($n = 9$), for 2, 7, 80, 125 and 250 μM Fe, respectively. Currents in the 80–250 μM range were not statistically different to the 7 μM Fe currents either. Nevertheless, currents recorded under 2 μM Fe were significantly different ($p < 0.05$) to than 7–250 μM Fe currents (Fig. 5b, dark bars). The mean capacitance values were 3.8 ± 0.45 pF ($n = 15$), 3.6 ± 0.57 pF ($n = 8$), 3.0 ± 0.68 pF ($n = 5$), 3.7 ± 0.35 pF ($n = 5$) and 5.6 ± 0.69 pF ($n = 9$), in cells treated with 2, 7, 80, 125, 250 μM Fe, respectively. These values are not statistically different to each other. Action potentials could be induced under all Fe concentrations tested in current clamp conditions upon the application of depolarizing current steps, after setting Vm to −80 mV by injecting hyperpolarizing current. The resting potential did not vary significantly within the 7–250 μM Fe. However, at 2 μM Fe the membrane potential (-8.09 ± 8.51 mV, $n = 11$) was significantly lower than at 7 μM (-20 ± 6 mV, $n = 8$)) ($p < 0.05$). Thus, concurrent with a less differentiated phenotype, cells treated with 2 μM Fe exhibited a significantly diminished membrane potential.

Discussion

An understanding of the processes allowing neuronal survival to high Fe concentrations may provide insights into the mechanisms of neuropathologies related to neuronal iron accumulation. To this end, we investigated the possible effect of prolonged Fe exposure on culture cells, using SHSY5Y cells as a model system.

Our data show that when SHSY5Y cells are subjected to increasing iron concentrations, their iron content increases, their viability decreases, and the cell sub-population that survives to high iron concentrations enters into a specific non-proliferative resting stationary phase or G_0. Surviving cells exhibited markers of neuronal differentiation and behaved as functional neurons according to electrophysiological parameters, as they were capable of firing action potentials. Because increases in cell iron content is accompanied by increased oxidative stress (Perry *et al*. 2000; Sayre *et al*. 2000; Núñez-Millacura *et al*. 2002; Doraiswamy and Finefrock 2004; Núñez *et al*. 2004), our results on cell death and survival need to be put into context of previous studies of cell survival during oxidative stress.

In terms of iron homeostasis, previous work has shown that the adaptation of SHSY5Y cells to an increasing iron load includes increases in the iron-storage protein ferritin and

the iron export transporter Ireg1, concomitant with a decrease in the iron import transporter DMT1 (Aguirre *et al*. 2005). Despite these adaptive strategies, cell iron content and ROS levels remain elevated. At the cellular level, ROS elicit a wide range of responses, ranging from cell proliferation, growth arrest and senescence, to apoptosis. In proliferating mammalian cells, these responses depend on the severity of the damage and on the cell type. At very low doses, 3–15 μM, hydrogen peroxide elicits a significant mitogenic response, whereas higher concentrations of H_2O_2, 120–150 μM, cause a temporary growth arrest in mammalian fibroblasts (Chen *et al*. 2000). Cells exposed to higher concentrations than those causing temporary arrest and transient adaptation can be forced into a permanent growth arrest state. Thus, cells exposed to H_2O_2 concentrations of 250–400 μM never divide again, and a fraction of cells exposed to 1.0 mM H_2O_2 become apoptotic. At even higher concentrations of hydrogen peroxide, cells simply disintegrate or become necrotic (Chen and Ames 1994; Wiese *et al*. 1995; Davies 1999; Chen *et al*. 2004).

Our data shows that treatment of SHSY5Y cells with iron concentrations above 80 μM Fe resulted in a 50% increase of cells in G_0. Insofar as the progression through the cell cycle is a tightly co-ordinated event, its proper regulation seems to be crucial for cell viability. In proliferating cells, checkpoints tightly control progress through the cell cycle. The transitions between these phases are mediated by heterodimeric kinases made of a regulatory subunit, cyclin, and a catalytic subunit, known as cyclin-dependent kinase or Cdk.

Another key mediator that may be mediating iron-induced oxidative stress damage is the tumor suppressor protein p53 (Agarwal *et al*. 1998). The amount of p53 increases in response to a variety of signals, such as damaged DNA, arrest of DNA or RNA synthesis, or nucleotide depletion. Upon DNA damage p53, acting as a transcription factor induces the synthesis of the repair proteins DDB2 and XPC (Ford 2005). An association between iron accumulation and p53 remains to be established.

The observation that cell division cycle 2 (cdc2), a cycle cell regulator, initiates apoptosis in post-mitotic neurons via direct activation of Bad, a trigger of apoptosis, indicates a direct interaction between the cell cycle machinery and the apoptotic program (Konishi *et al*. 2002). In fact, activation of some cell cycle proteins that give rise to aborted cell cycle entry have been observed in dying neurons of brains with neurodegenerative disorders (Husseman *et al*. 2000; Liu and Greene 2000; Yang *et al*. 2001; Yang *et al*. 2003). This indicates the existence of an exquisite fine-tuning of cell cycle by the oxidative stress response, which may lead to apoptosis (Klein and Ackerman 2003; Becker and Bonni 2004; Herrup *et al*. 2004; Kruman 2004), although there is some evidence that the neuronal death may be cell cycle-independent (Langley and Ratan 2004). In this context, our observation that iron induced entrance into G_0 may be seen as an intermediate step where live, functional neurons successfully adapt to oxidative stress.

An indication that the cell cycle state adopted by the SHSYSY cells may be a response to Fe-induced oxidative stress was provided by microarray studies showing that in response to iron accumulation, cyclin G_1 and Hsp90 were up-regulated in these cells (Mura and Núñez, unpublished results). Hsp90 belongs to a family of heat shock proteins which are induced in response to stress conditions such as high temperature. Heat shock and oxidative stress, among other forms of stress, has been shown to suppress cell growth by inhibiting cell cycle transitions and inducing cell death (Nakai and Ishikawa 2001; Burrows *et al*. 2004). The change in gene expression of Hsp90 therefore indicates an early response to oxidative stress probably associated with changes in the cell cycle. This conclusion was supported by the observed cyclin G_1 up-regulation (Zhao *et al*. 2003).

Our data shows that the sub-population of SHSY5Y cells surviving high Fe exposure display expression of MAP-2 and tau proteins, indicating that the cells have reached a terminal differentiation state. It is generally accepted that terminal differentiation of neuroblasts occurs once they are arrested in G_0 (reviewed by Ross 1996). The surviving sub-population of SHSY5Y cells arrested in G_0, and showing markers of terminal differentiation, behaved like functional neurons, as indicated by the electrophysiological experiments. We have used the resting potential, the ability to fire action potentials and the voltage-dependent inward and outward currents as parameters indicating cell membrane integrity and the functionality of membrane components such as ion channels and ion pumps. In cells cultured under iron-deficient conditions (2 μM), the resting potential was reduced to 40% of the value measured in cells treated with normal iron concentration (7 μM), in spite of the fact that the current amplitudes were not significantly different from those observed in normal iron concentration. The large standard deviation and a distribution analysis (data no shown) of the outward current amplitudes measured in 2 μM Fe suggests the presence of more than one cell sub-population. Cells challenged with iron concentrations higher than 250 μM presented the same resting potential values and outward currents as cells grown in normal (7 μM) iron concentrations, suggesting that the high iron population have a normal electrical behavior. These results indicate that the Fe treatment commits a fraction of proliferative, undifferentiated SHSY5Y cells to a neuronal phenotype, suggesting that Fe treatment may be mimicking some of the developmental signals that commit pluripotential neural crest cells to a neuronal fate.

Taking all these results together, we conclude that the adaptation of the SHSY5Y cells to oxidative stress is related to a change in cell cycle. Cell viability decreases at high iron concentrations, but the surviving cell sub-population is more homogenous in terms of its phenotype, quiescence,

electrophysiological properties, and expression of the neuronal markers MAP2 and tau. According to the electrophysiological properties, the adapted cell sub-population resembles normal differentiated neurons. This also indicates that the iron-induced oxidative stress produced a quiescent cell sub-population capable of handling oxidative stress.

Our results agree with previous studies on cultured mammalian cells, which showed that fibroblasts can survive for several weeks after exposure to 100–200 μM H_2O_2 without dividing again (Davies 1999). They are also consistent with reports describing a relationship between quiescent state, anti-oxidative defense and cell survival (Chen *et al*. 2000; Naderi *et al*. 2003; Ekshyyan and Aw 2005). Interestingly in yeast, a novel kinase, Rim 15, has been implicated in the integration of nutrient and oxidative stress signals to trigger a transcriptional program that leads to cell survival in G_0 for an extended period of time (Cameroni *et al*. 2004).

It has been proposed that the level of oxidative stress may determine which pathway(s) is induced (Martindale and Holbrook 2002). Reactive oxygen species produced as intermediates of iron induced oxidative stress, would lead to a state of cell cycle arrest, maintaining the cells alive. Reactive oxygen species could serve as messengers to trigger an endogenous program of cell death that may be promoted by multiple pathways (Langley and Ratan 2004). The final fate of the cell, life or death, would depend on the level, type or duration of oxidative stress and, more importantly, on the strength of the endogenous antioxidant mechanisms.

Acknowledgements

This work was supported by MIDEPLAN ICM P99–031F

We want to thank Christian Gonzalez-Billaut for providing the anti-MAP-2 and the antitau antibodies and Dr Maria Ines Becker for the secondary HPR antibodies. We are also grateful to Dr Jose Minguel for critical reading of the manuscript.

References

Agarwal M. L., Taylor W. R., Chernov M. V., Chernova O. B. and Stark G. R. (1998) The p53 network. *J. Biol. Chem.* **273**, 1–4.

Aguirre P., Mena N., Tapia V., Arredondo M. and NuneZ. M. T. (2005) Iron homeostasis in neuronal cells: a role for IREG1. BMC Neurosci. 6, article 3.

Andersen J. K. (2004) Oxidative stress in neurodegeneration: cause or consequence? *Nat Rev. Neurosci. [(Suppl.)]* **10**, S18–S25.

Barnham K. J. Masters C. L. & Bush A. I. (2004) Neurodegenerative diseases and oxidative stress. Nat. Rev. Drug Discov. 3, 205–214.

Bazan N. G. (2003) Synaptic lipid signaling: significance of polyunsaturated fatty acids and platelet-activating factor. *J. Lipid Res.* **44**, 2221–2233.

Becker E. B. E. and Bonni A. (2004) Cell cycle regulation of neuronal apoptosis in development and disease. *Prog. Neurobiol.* **72**, 1–25.

Burrows F., Zhang H. and Kamal A. (2004) Hsp90 activation and cell cycle regulation. *Cell Cycle* **3**, 1530–1536.

Cameroni E., Hulo N., Roosen J., Winderrickx J. and De Virgilio C. (2004) The novel Yeast PAS kinase orchestrates G_0-associated antioxidant defense mechanisms. *Cell Cycle* **3**, 462–468.

Chen Q. and Ames B. N. (1994) Senescence-like growth arrest induced by hydrogen peroxide in human fibroblast F65 cells. *Proc. Natl. Acad. Sci. U.S.A.* **91**, 4130–4134.

Chen Q. M., Liu J. and Merrett J. B. (2000) Apoptosis or senescence-like growth arrest: influence of cell-cycle position, p53, 21 and bax in H_2O_2 response of normal human fibroblasts. *Biochem. J.* **347**, 543–551.

Chen J.-H., Stoeber K., Kingsbury S., Ozanne S. E., Williams G. H. and Hales C. N. (2004) Loss of proliferantive capacity and induction of senescence in oxidatively stressed human fibroblasts. *J. Biol. Chem.* **279**, 49 439–49 446.

Davies K. J. A. (1999) The broad spectrum of responses to oxidants in proliferating cells: a new paradigm for oxidative stress. *Life* **48**, 41–47.

Doraiswamy P. M. and Finefrock A. E. (2004) Metals in our minds: therapeutic implications for neurodegenerative disorders. *Lancet Neurol.* **3**, 431–434.

Ekshyyan O. and Aw T. Y. (2005) Decreased susceptibility of differentiated PC12 cells to oxidative challenge: relationship to cellular redox and expression of apoptotic protease activator factor-1. *Cell Death Differentiation* **12**, 1066–1077.

Encinas M., Iglesias M., Liu Y., Wang H., Muhaisen A., Ceña V., Gallego C. and Comella J. X. (2000) Sequential treatment of SHSY5Y cells with retinoic acid and brain-derived neurotrophic factor-dependent, human neuron-like cells. *J. Neurochem.* **75**, 991–1003.

Ford J. M. (2005) Regulation of DNA damage recognition and nucleotide excision repair: another role for p53. *Mutat. Res.* **577**, 195–202.

Fukuyama F., Nakayama A., Nakase T., Toba H., Mukainaka T., Sakaguchi H., Saikawi T., Sakurai H., Wada M. and Fushiki S. (2002) A newly established neuronal ρ-0 cell line highly susceptible to oxidative stress accumulates iron and other metals. *J.Biol. Chem.* **277**, 41 455–41 462.

Gotz M. E., Double K., Gerlach M., Youdim M. B. and Riederer P. (2004) The relevance of iron in the pathogenesis of Parkinson's disease. *Ann. N Y Acad. Sci.* **1012**, 193–208.

Griffiths P. D., Dobson B. R., Jones G. R. and Clarke D. T. (1999) Iron in the basal ganglia in Parkinson's disease. An in vitro study using extended X-ray absorption fine structure and cryo-electron microscopy. *Brain* **122**, 667–673.

Gross S. S. and Levi R. (1992) Tetrahydrobiopterin synthesis: an absolute requirement for cytokine-induced nitric oxide generation by vascular smooth muscle. *J.Biol. Chem.* **267**, 25 722.

Hald A. and Lotharius J. (2005) Oxidative stress and inflammation in Parkinson's disease: Is there a causal link? . *Exp Neurol.* **193**, 279–290.

Herrup K., Neve R., Ackerman S. L. and Copani A. (2004) Divide and Die: Cell cycle events as triggers of nerve cell death. *The. J. Neuroscience* **24**, 9232–9239.

Husseman J. W., Nochlin D. and Vincent I. (2000) Mitotic activation: a convergent mechanism for a cohort of neurodegerative diseases. *Neurobiol. Aging* **21**, 815–828.

Jenner P. and Olanow C. W. (1996) Oxidative stress and the pathogenesis of Parkinson's diseases. *Neurology* **47**, S161–S170.

Kim M., Cooper D. D., Hayes S. F. and Spangrude G. J. (1998) Rhodamine-123 staining in hematopoietic stem cells of young mice indicates mitochondrial activation rather than dye efflux. *Blood* **91**, 4106.

Klein J. A. and Ackerman S. L. (2003) Oxidative stress, cell cycle and neurodegeneration. *J. Clin. Invest.* **111**, 785–793.

Konishi Y., Lehtinen M., Donovan N. and Bonni A. (2002) Cdc2 phosphorylation of BAD links the cell cycle to the cell death machinery. *Mol. Cell* **9**, 1005–1016.

Kruman I. I. (2004) Why do neurons enter the cell cycle. *Cell Cycle* **3**, 769–773.

Langley B. and Ratan R. R. (2004) Oxidative-stress induced death in the nervous system: cell cycle dependent or independent? . *J. Neuroscience Res.* **77**, 621–629.

Liu D. X. and Greene L. A. (2000) Regulation of neuronal survival and death by E2F-dependent gene repression and derepression. *Neuron* **32**, 425–438.

Martell A. E. and Smith, R. M., ed. (2004). *Institute of Standards and Technology (NIST) Critically Selected Stability Constants of Metal Complexes.* 46. NIST Standard Reference Database, Boulder, CO, USA.

Martindale J. L. and Holbrook L. J. (2002) Cellular response to oxidative stress: signaling for suicide and Survival. *J. Cellular Physiol.* **192**, 1–15.

Mura C. V., Cosmelli D., Muñoz. F. and Delgado R. (2004) Orientation of Arabidopsis thaliana KAT1 channel in the plasma membrane. *J. Memb. Biol.* **201**, 157–165.

Naderi J., Hung M. and Pandey S. (2003) Oxidative stress-induced apoptosis in dividing fibroblasts involve activation of p38 MAP kinase and over-expression of Bax: resistance of quiescent cells to oxidative stress. *Apoptosis* **8**, 91–100.

Nakai A. and Ishikawa T. (2001) Cell cycle transition under stress conditions controlled by vertebrate heat shock factors. *The EMBO J.* **20**, 2885–2895.

Núñez M. T., Gallardo V., Muñoz. P., Tapia V., Esparza A., Salazar J. and Speisky H. (2004) Progressive iron accumulation induces a biphasic change in the glutathione content of neuroblastoma cells. *Free Rad. Biol. Med.* **37**, 953–960.

Núñez-Millacura C., Tapia V., Muñoz. P., Maccioni R. B. and Núñez M. T. (2002) An oxidative stress-mediated positive-feedback iron uptake loop in neuronal cells. *J. Neurochem.* **82**, 240–248.

Pahlman S., Hoehner J. C., Nanberg E., Hedborg F., Fagerstrom S., Gestblom C., Johansson I., Larsson U., Lavenius E., Ortoft E. *et al.* (1995) Differentiation and survival influences of growth factor in human neuroblastoma. *Eur. J. Cancer* **31**, 453–458.

Perry G., Raina A. K., Nunomura A., Wataya T., Sayre L. M. and Smith M. A. (2000) How important is oxidative damage? Lessons from Alzheimer's disease. *Free Radic. Biol. Med.* **28**, 831–834.

Ross M. E. (1996) Cell division and the Nervous system: regulating the cycle from neural differentiation to death. *TINS* **19**, 62–68.

Ross R. A., Spengler B. A. and Biedler J. L. (1983) Coordiante morphological interconversion of human neuroblatoma. *J. Natl. Cancer Inst.* **71**, 741–747.

Sayre L. M., Perry G., Atwood C. S. and Smith M. A. (2000) The role of metals in neurodegenerative diseases. *Cell. Mol. Biol.* **46**, 731–741.

Sokoloff L. (2000) In vivo veritas: probing brain function through the use of quantitative in vivo biochemical techniques. *Ann. Rev. Physiol.* **62**, 1–24.

Wiese A. G., Pacifici R. E. and Davies K. J. A. (1995) Transient adaptation of oxidative stress in mammalian cells. *Arch. Biochem. Biophys.* **318**, 231–240.

Wolf N. S., Kone A., Priestley G. V. and Bartelmez. S. H. (1993) In vivo and in vitro characterization of long-term repopulating primitive hematopoietic cells isolated by sequential Hoechst 33342-rhodamine 123 FACS selection. *Exp Hematol.* **21**, 614.

Yang Y., Geldmacher D. S. and Herrup K. (2001) DNA replication precedes neuronal cell death in Alzheimer's disease. *J. Neurosci.* **21**, 2661–2668.

Yang Y., Mufson E. J. and Herrup K. (2003) Neuronal cell death is preceded by cell cycle events at all stages of Alzheimer's disease. *J. Neurosc.* **23**, 2557–2563.

Youdim M. B. and Riederer P. (1993) The role of iron in senescence of dopaminergic neurons in Parkinson's disease. *J. Neural Transm-supplement* **40**, 57–67.

Zecca L., Gallorini M., Schünemann V., Alfred X., Trautwein A. X., Gerlach M., Riederer P., Vezzoni P. and Tampellini D. (2001) Iron, neuromelanin and ferritin content in the substantia nigra of normal subjects at different ages: consequences for iron storage and neurodegenerative processes. *J. Neurochem.* **76**, 1766–1773.

Zecca L., Youdim M. B., Riederer P., Connor J. R. and Crichton R. R. (2004) Iron, Brain Ageing and Neurodegerative Disorders. *Nature Rev./Neuroscience* **5**, 863–873.

Zhao L., Samuels T., Winckler S., Korgaonkar C., Tompkins V., Horne M. C. and Quelle D. E. (2003) Cyclin G1 has growth inhibitory activity linked to the ARF-Mdm2-p53 and pRb tumor suppressor pathways. *Mol. Cancer Res.* **1**, 195–206.